A method based on diffraction theory for predicting 3D focusing performance of compound refractive X-ray lenses

Zichun Le (乐孜纯)[1], Kai Liu (刘 恺)[1], and Jingqiu Liang (梁静秋)[2]

[1] *College of Information Engineering, Zhejiang University of Technology, Hangzhou 310032*

[2] *State Key Laboratory of Applied Optics, Changchun Institute of Optics, Fine Mechanics and Physics, Chinese Academy of Sciences, Changchun 130022*

Received October 10, 2004

A method based on the diffraction theory for estimating the three-dimensional (3D) focusing performance of the compound refractive X-ray lenses is presented in this paper. As a special application, the 3D X-ray intensity distribution near the focus is derived for a plano-concave compound refractive X-ray lens. Moreover, the computer codes are developed and some results of 3D focusing performance for a compound refractive X-ray lens with Si material are shown and discussed.

OCIS codes: 340.0340, 260.1960, 110.0110.

In 1996, a new X-ray optical device named the compound refractive X-ray lens was developed[1], and it was used in an experimental system for focusing a 14-keV X-ray beam to an 8-μm spot. Soon after, many studies about it appeared, including the theories[2−5], the fabrication technologies[6,7], and the experimental X-ray analysis systems[8−10] based on the compound refractive X-ray lenses such as X-ray microscope, X-ray fluorescence, X-ray micro-beam applications, etc.. The compound refractive X-ray lens works in the case of X-rays with energy larger than 5-keV (hard X-rays). Its alignment in the X-ray beam is easier due to its straight optical path. Furthermore, it is very robust, compact, and easy to handle. Therefore the compound refractive X-ray lens is very attractive for the development of X-ray analytical investigations with a spatial resolution in the micrometer and sub-micrometer range.

The research results on the focusing performances in the focal plane and the transmission efficiency of the compound refractive X-ray lenses have been analyzed[2−5]. However there has been little work concerning the three-dimensional (3D) focusing behavior of such a device. In order to obtain a fuller understanding of the focusing performances of compound refractive X-ray lenses, not only the X-ray distribution in the focal plane, but also that in the neighborhood of this plane must be studied. Furthermore, the knowledge of the 3D distribution near focus is of particular importance in estimating the tolerance in the setting of the receiving plane in an X-ray image-forming system. As a special application, the 3D X-ray intensity distribution near the focus is derived for the compound refractive X-ray lenses with plano-concave elementary lenses in this letter. The introduced theoretical method can be easily generalized to other compound refractive lenses with different structures such as double-concave elementary lenses.

Consider a compound refractive X-ray lens composed of a group of N plano-concave elementary lenses positioned in line with axial symmetry, as shown in Fig. 1. In the figure, R stands for the radius of the concave surface, d and t are the center thickness and the edge thickness of the elementary lens respectively, and $D(r)$ is the thickness function introduced in Ref. [11]. In general, the length of a compound refractive X-ray lens is much shorter than its focal length, therefore the compound refractive X-ray lens can be considered as a thin lens. Here we define a diffractive screen function $H_N(r) = [\tau(r) \cdot A(r)]^N$, which describes the transmittance function of the compound refractive X-ray lenses by taking account of both the refraction effect and absorption, N stands for the number of the elementary lenses, $A(r)$ and $\tau(r)$ are responsible accordingly for the attenuation coefficient and the transmission coefficient respectively,

$$\tau(r) = \exp\left[i\frac{2\pi}{\lambda}(t-\delta d)\right]\exp\left[-i\frac{\pi\delta r^2}{\lambda R}\right], \tag{1}$$

$$\begin{aligned} A(r) &= \exp\left[-\frac{4\pi\beta}{\lambda}D(r)\right] \\ &= \exp\left[-\frac{4\pi\beta d}{\lambda}\right]\exp\left[-\frac{2\pi\beta r^2}{\lambda R}\right], \end{aligned} \tag{2}$$

where λ stands for the wavelength of incident X-ray radiation, β and δ are related to absorption and refraction respectively in the expression ($\tilde{n} = 1 - \delta - i\beta$) of the optical constant in X-ray region. Therefore the diffractive screen function can be rewritten as

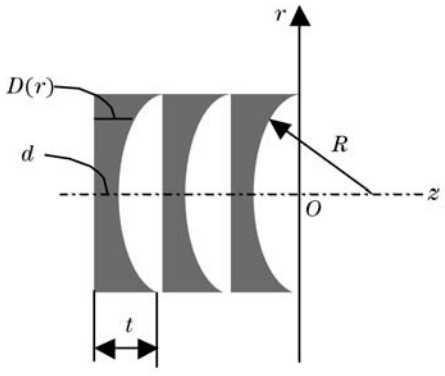

Fig. 1. Scheme of a compound refractive X-ray lens.

$$\begin{cases} H_N(r) = C_1 \exp\left[-\frac{2\pi\beta N r^2}{\lambda R}\right] \exp\left[-i\frac{\pi\delta N r^2}{\lambda R}\right] \\ C_1 = \exp\left[-\frac{4\pi\beta dN}{\lambda}\right] \exp\left[i\frac{2\pi}{\lambda}(t-\delta d)N\right] \end{cases}. \quad (3)$$

Because the compound refractive X-ray lenses were usually used in the experimental systems with the synchrotron radiation source, which is considered as a source of low emittance, high flux, and high brilliance, the incident wave on the compound lenses can be regarded as a plane monochromatic X-ray wave. Therefore, the complex amplitude of the point (ρ, z) in the image region can be calculated according to Kirchhoff integral within the Fresnel approximation[12],

$$U(\rho,z) = C_2 \iint_{H_N} H_N(r) \exp\left(ik\frac{r^2}{2z}\right) \exp\left[-ik(p_1 x + q_1 y)\right] \mathrm{d}x\mathrm{d}y, \quad (4)$$

where z is the coordinate along the optical axis, (x, y) stands for the point r in the object plane and (x_1, y_1) is the point ρ at the receiving plane in the image region. (p_1, q_1) stands for the direction cosine of the refracted ray, and we have $p_1 \cong \frac{x_1}{z}$, $q_1 \cong \frac{y_1}{z}$. C_2 is a complex constant. By introducing polar coordinates and substituting Eq. (3) into Eq. (4), we have

$$U(\rho,z) = C_1 C_2 \int_0^\infty \exp\left(-\frac{2\pi\beta N r^2}{\lambda R}\right) \exp\left[i\frac{\pi r^2}{\lambda}\left(\frac{1}{z}-\frac{\delta N}{R}\right)\right] J_0\left(\frac{2\pi}{\lambda z} r\rho\right) r\mathrm{d}r. \quad (5)$$

As far as the X-ray 3D distribution near focus is concerned, Eq. (5) can be approximated to the following equation by using the expression of the focal length of the compound refractive X-ray lens $f = R/N\delta$,

$$U(\rho,\Delta z) \cong C_1 C_2 \int_0^\infty \exp\left[-\frac{2\pi\beta N r^2}{\lambda R}\right] \exp\left[i\frac{\pi r^2}{\lambda f^2}\Delta z\right] J_0\left(\frac{2\pi\rho}{\lambda f} r\right) r\mathrm{d}r, \quad (6)$$

where $\Delta z = f - z$ is used to stand for the distance departure from the focus along the optical axis. It is obvious therefore from Eq. (6) that the axial and transverse behaviors are not independent. By means of some complicated mathematical derivations, we finally obtain the expression of the 3D X-ray intensity distribution near focus as

$$I(\rho,\Delta z) = |C_1 C_2|^2 \frac{4\pi^2\beta^2 N^2\lambda^2 R^2 + \lambda^4 R^4 \nu^2}{\left[8\pi^2\beta^2 N^2 + 2\lambda^2 R^2 \nu^2\right]^2} \exp\left[-\frac{\pi\beta\lambda N R\alpha^2}{4\pi^2\beta^2 N^2 + \lambda^2 R^2 \nu^2}\right], \quad (7)$$

where

$$\begin{cases} \alpha = \frac{2\pi\rho}{\lambda f} = \frac{2\pi N\delta}{\lambda R}\sqrt{x^2+y^2} \\ \nu = \frac{\pi(\Delta z)}{\lambda f^2} = \frac{\pi N^2\delta^2}{\lambda R^2}(\Delta z) \end{cases}. \quad (8)$$

From Eq. (7), we can see that the 3D focusing performance of the compound refractive X-ray lens is relative to the parameters of the lens including its working wavelength (λ), material (β and δ) of the lens, and the structural parameters of the lens such as the number (N) of elementary lenses and the radius (R) of concave surface. Moreover, the normalized 3D intensity distribution near focus can be expressed as

$$I(\rho,\Delta z)/I(0,0) = \frac{64\pi^4\beta^4 N^4 + 16\pi^2\beta^2 N^2\lambda^2 R^2\nu^2}{\left[8\pi^2\beta^2 N^2 + 2\lambda^2 R^2\nu^2\right]^2} \exp\left[-\frac{\pi\beta\lambda N R\alpha^2}{4\pi^2\beta^2 N^2 + \lambda^2 R^2\nu^2}\right]. \quad (9)$$

A comparison between the index of refraction (δ) and the index of absorption (β) for the high-energy X-rays (> 5 keV) shows that the low-Z materials (such as Al, Be, Li, B, and Si) seem more suitable for fabricating the compound X-ray refractive lenses[6]. Here we choose Si material as an example material for the lens. Besides the advantage of small absorption of low-Z materials, Si compound refractive lens is also easy to fabricate by means of standard microfabrication techniques. According to the theoretical results introduced above, a general prediction on the 3D focusing performance has been given for a Si compound refractive X-ray lens whose parameters are: working wavelength of 0.04 nm, geometrical aperture of 1 mm, length of the lens around 50 mm, and focal length of the lens of 9.9 m. A 3D intensity plot near focus of the Si compound refractive X-ray lens is shown in Fig. 2. The normalized intensity is shown along the z-direction. In addition, x and y stand for the axial and the transverse directions, respectively, $x = \frac{\pi N^2\delta^2}{\lambda R^2}(\Delta z)$ is with unit of mm^{-2} and $y = \frac{2\pi N\delta}{\lambda R}\rho$ is with unit of mm^{-1}.

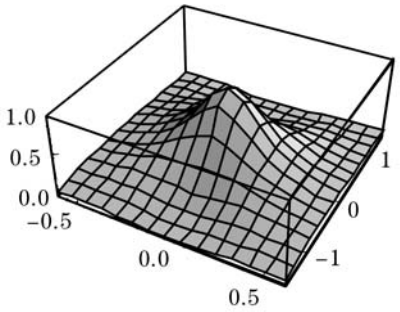

Fig. 2. Normalized 3D intensity distribution near the focus for Si compound refractive X-ray lens with $\lambda = 0.04$ nm, $R = 500$ μm, $N = 100$.

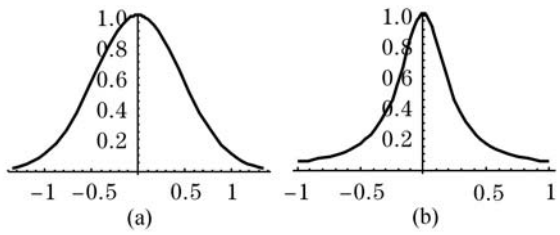

Fig. 3. Normalized transverse (a) and axial (b) intensity distributions for Si compound refractive X-ray lens with $\lambda = 0.04$ nm, $R = 500$ μm, $N = 100$.

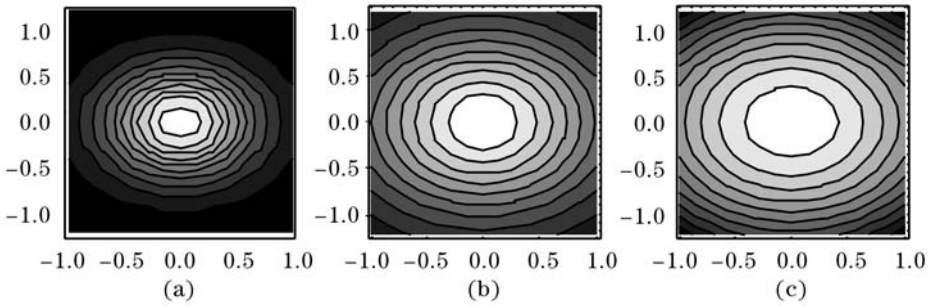

Fig. 4. Intensity distributions at different receiving planes along the optical axis for Si compound refractive X-ray lens with $\lambda = 0.04$ nm, $R = 500$ μm, $N = 100$. (a) At the focal plane; (b) at $\Delta z = \pm 3.7773$ cm; (c) at $\Delta z = \pm 12.5911$ cm.

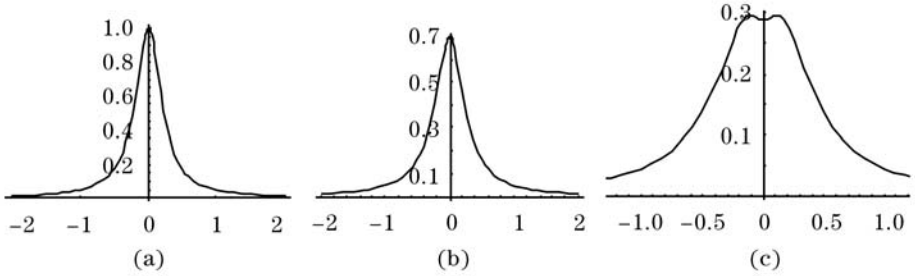

Fig. 5. Intensity distributions along the axis (a), at the planes with $\rho = \pm 0.2532$ μm (b) and $\rho = \pm 0.4748$ μm (c) of Si compound refractive X-ray lens with $\lambda = 0.04$ nm, $R = 500$ μm, $N = 100$.

In order to see the details on the focal behavior near the focal point, the normalized transverse intensity distribution of the Si compound refractive X-ray lens is shown in Fig. 3(a). In addition, Fig. 3(b) shows the normalized axial intensity distribution. Figure 4 is drawn for the normalized intensity distributions at different receiving planes along the optical axis, Figs. 4(a), (b), and (c) show the contour plots for the intensity distribution at the focal plane, at the receiving plane $\Delta z = \pm 3.7773$ cm, and at the receiving plane $\Delta z = \pm 12.5911$ cm, respectively. It is clear that the focal beam disperses rapidly when the receiving planes are departure from the focal plane. Figure 5 shows the intensity distributions along the axis, at the planes with $\rho = \pm 0.2532$ μm, and $\rho = \pm 0.4748$ μm. It is clear that the X-ray intensity decreases rapidly when the observed points are away from the focus.

From the calculation results and the figures shown above, we can conclude that the 3D focusing performance of the compound refractive X-ray lenses can be predicted by the theoretical method introduced in this paper. Moreover the information for the 3D intensity distribution near focus is of particular importance for designing and establishing an X-ray imaging system based on the compound refractive X-ray lenses. However, the derivation of the 3D X-ray intensity distribution near focus is quite complicated, a simpler method is needed to work out in further research.

This work was supported by the National Natural Science Foundation of China (No. 10174079) and the fund for the qualified researchers in the Zhejiang University of Technology, P. R. China. Z. Le's e-mail address is lzc@zjut.edu.cn.

References

1. A. Snigirev, V. Kohn, I. Snigireva, and B. Lengeler, Nature **384,** 49 (1996).
2. Z. Le and J. Liang, J. Opt. A: Pure and Appl. Opt. **5,** 374 (2003).
3. J. Ye, Z. Le, J. Liang, K. Liu, B. Quan, Y. Qin, and G. Zhu, Chin. Opt. Lett. **2,** 367 (2004).
4. V. V. Protopopov and K. A. Valiev, Opt. Commun. **151,** 297 (1998).
5. B. Lengeler, J. Tümmler, A. Snigirev, I. Snigireva, and C. Raven, J. Appl. Phys. **84,** 5855 (1998).
6. A. Snigirev, V. Kohn, I. Snigireva, A. Souvorov, and B. Lengeler, Appl. Opt. **37,** 653 (1998).
7. A. Snigirev, B. Filseth, P. Elleaume, Th. Klocke, V. Kohn, B. Lengeler, I. Snigireva, A. Souvorov, and J. Tuemmler, Proc. SPIE **3151,** 164 (1997).
8. B. Lengeler, C. G. Schroer, M. Richwin, J. Tümmler, M. Drakopoulos, A. Snigirev, and I. Snigireva, Appl. Phys. Lett. **74,** 3924 (1999).
9. D. A. Arms, E. M. Dufresne, R. Clarke, S. B. Dierker, N. R. Pereira, and D. Foster, Rev. Sci. Instru. **73,** 1492 (2002).
10. S. Bohic, A. Simionovici, A. Snigirev, R. Ortega, G. Devès, D. Heymann, and C. Schroer, Appl. Phys. Lett. **78,** 3544 (2001).
11. J. W. Goodman, *Introduction to Fourier Optics* (2nd edition) (McGraw-Hill, New York, 1996) p.96.
12. M. Born and E. Wolf, *Principles of Optics* (7th edition) (Cambridge University Press, Cambridge, UK, 1999) p.484.